CIA Open Access

Energy-Aware Scheduling Algorithm Optimization for AI Workloads in Data Centers Based on Renewable Energy Supply Prediction

Xiaoying Li[1], Ruoxi Jia[1.2]

[1] Carnegie Mellon University, M.S. in Software Engineering, Mountain View, CA, USA
[1.2] Computer Science, Universtiy of Southern California, CA, USA

DOI: 10.63575/CIA.2024.20206

Abstract

This paper presents an innovative energy-aware scheduling algorithm that optimizes artificial intelligence workload distribution in data centers through advanced renewable energy supply forecasting. The proposed system integrates a hybrid LSTM-GRU neural network architecture, achieving a correlation coefficient of 0.87 for 24-hour renewable energy forecasts with a mean absolute error of 13%. Our priority-aware scheduling mechanism dynamically categorizes AI workloads based on energy intensity and deadline constraints, enabling optimal alignment with fluctuating renewable energy resources. Experimental evaluation across three geographically distributed data centers over a 12-month period demonstrates measurable improvements: 58% reduction in grid energy dependency, 47% decrease in carbon emissions, and 34% reduction in operational costs while maintaining 96.2% service level agreement compliance. The system architecture employs multi-objective optimization techniques, balancing energy efficiency, performance metrics, and carbon footprint considerations.

Keywords: *Energy-Aware Scheduling, Renewable Energy Prediction, Sustainable Computing, AI Workload Management*

1. Introduction

1.1 Background and Motivation

The exponential growth of artificial intelligence applications has fundamentally transformed computational requirements in modern data centers. Training large-scale machine learning models now consumes hundreds of megawatt-hours of electricity, with GPT-3 training alone requiring 1,287 MWh, equivalent to the annual consumption of 120 American homes. Data centers currently account for approximately 1.8% of global electricity consumption, projected to reach 3.2% by 2030. This unprecedented energy demand creates substantial environmental impacts, with the information and communication technology sector contributing 4% of global greenhouse gas emissions.

The integration of renewable energy sources presents both opportunities and challenges for sustainable data center operations. Solar and wind energy costs have decreased by 89% and 69% respectively over the past decade, making renewable sources economically viable. GPU dynamic voltage and frequency scaling (DVFS) technologies enable fine-grained power management, as demonstrated in comprehensive surveys showing 15-30% energy savings potential [1]. The variability of renewable energy generation necessitates sophisticated prediction and scheduling mechanisms to maintain operational efficiency while maximizing green energy utilization.

1.2 Research Challenges

The intermittent nature of renewable energy sources creates significant scheduling complexities. Solar energy availability follows diurnal patterns with weather-dependent variations reaching 70% deviation from forecasted values during storm events. Wind power exhibits even greater unpredictability, with hour-to-hour fluctuations exceeding 40% of rated capacity. These uncertainties compound when managing heterogeneous AI workloads with diverse computational patterns, memory requirements, and deadline constraints.

The multi-objective optimization problem involves minimizing energy consumption, reducing carbon emissions, maintaining quality of service, and controlling operational costs simultaneously. Particle swarm optimization and genetic algorithms have shown promise in solving similar complex optimization problems, with comparative studies demonstrating PSO's superior convergence speed in high-dimensional spaces [2]. The computational complexity increases exponentially with the number of tasks and resources, requiring efficient approximation algorithms for real-time decision making.

1.3 Contributions and Paper Organization

This research presents three primary contributions advancing the state of sustainable AI computing. A novel hybrid LSTM-GRU prediction framework achieves improved accuracy in multi-horizon renewable energy forecasting through integration of satellite imagery, numerical weather predictions, and historical generation patterns. The priority-aware scheduling algorithm introduces dynamic workload categorization with mathematical guarantees for deadline compliance while maximizing renewable energy utilization. Comprehensive experimental validation across geographically distributed data centers provides empirical evidence of the system's effectiveness in production environments.

The paper organization follows a structured approach to presenting these contributions. Section 2 examines related work in renewable energy prediction, scheduling algorithms, and carbon-aware computing frameworks. Section 3 details the system architecture and algorithm design, including the mathematical formulation and optimization strategies. Section 4 presents experimental evaluation results demonstrating significant improvements in energy efficiency and carbon reduction. Section 5 concludes with summary insights and future research directions.

2. Related Work and State-of-the-Art

2.1 Renewable Energy Prediction Models

Traditional statistical approaches for renewable energy forecasting rely on autoregressive integrated moving average (ARIMA) models and exponential smoothing techniques. These methods achieve acceptable accuracy for short-term predictions under stable weather conditions but fail to capture non-linear patterns inherent in atmospheric dynamics. Linear regression models incorporating weather features provide baseline predictions with mean absolute errors ranging from 15% to 25% for 24-hour horizons.

Deep learning architectures have improved renewable energy forecasting accuracy. Joint exploration of CPU-memory DVFS demonstrates the interconnected nature of energy optimization across system components [3]. Long short-term memory networks process temporal sequences effectively, achieving correlation coefficients of 0.92 for solar irradiance prediction. Gated recurrent units reduce computational overhead while maintaining comparable accuracy, which is particularly beneficial for edge deployment scenarios. Transformer architectures with attention mechanisms capture long-range dependencies in weather patterns, improving multi-day forecast reliability by 23% compared to recurrent models.

2.2 Energy-Aware Scheduling Algorithms

The evolution of energy-aware scheduling has progressed from simple heuristics to sophisticated optimization frameworks. The application of PSO and genetic algorithm techniques in demand estimation problems demonstrates their effectiveness in handling non-linear optimization landscapes [4]. Energy-aware non-preemptive task scheduling with deadline constraints in DVFS-enabled heterogeneous clusters achieves a 35% energy reduction while meeting timing requirements [5]. The integration of machine learning predictions with scheduling decisions enables proactive resource allocation based on anticipated workload patterns.

Meta-heuristic approaches provide near-optimal solutions for NP-hard scheduling problems. Multi-objective optimization using particle swarm optimization balances competing objectives through Pareto frontier exploration [6]. Genetic algorithms with specialized crossover operators preserve solution feasibility while exploring the search space efficiently. Hybrid approaches combining multiple meta-heuristics leverage complementary strengths, achieving superior performance compared to individual techniques.

2.3 Carbon-Aware Computing Frameworks

Industry initiatives have established foundations for carbon-aware computing infrastructure. The Green Software Foundation's Carbon-Aware SDK provides standardized interfaces for accessing real-time carbon intensity data across global electricity grids. Microsoft's collaboration with UBS demonstrates practical implementation, achieving a 15% reduction in software carbon intensity through temporal workload shifting. Google's power-first development prioritizes locations with abundant renewable energy access, reducing operational carbon footprints by 40%.

Academic contributions advance theoretical understanding and practical implementations of carbon-aware systems. The Carbon Explorer framework provides holistic carbon accounting across hardware lifecycle, operational energy, and embodied emissions. CAFE introduces carbon-aware federated learning protocols that minimize carbon emissions during distributed model training. The Ecovisor virtual energy system abstraction enables transparent carbon optimization without application modifications. Recent standardization efforts establish the Software Carbon Intensity metric as SCI = ((E × I) + M) / R, where E represents energy consumption, I denotes carbon intensity, M accounts for embodied emissions, and R normalizes per functional unit.

3. System Architecture and Algorithm Design

3.1 System Overview and Components

3.1.1 Multi-layer Architecture Design

The system architecture implements a four-layer hierarchical design enabling modular functionality and scalability. The presentation layer exposes RESTful APIs supporting JSON and Protocol Buffer formats for client interactions. Web interfaces provide real-time monitoring dashboards displaying energy consumption, renewable availability, and workload distribution metrics. The business logic layer encapsulates scheduling algorithms, prediction models, and optimization routines within containerized microservices. Improving GPGPU energy-efficiency through concurrent kernel execution and DVFS requires coordinated management across architectural layers [7].

The data layer employs time-series databases optimized for high-frequency sensor readings and prediction model outputs. InfluxDB stores renewable energy measurements with nanosecond precision timestamps, supporting aggregation queries across multiple time windows. MongoDB maintains workload metadata, scheduling decisions, and system configuration parameters. The infrastructure layer interfaces directly with compute resources through vendor-specific APIs and hardware management protocols. Integration with NVIDIA Data Center GPU Manager enables fine-grained power monitoring and DVFS control at 100ms intervals.

3.1.2 Data Flow and Communication Protocols

Event-driven architecture facilitates asynchronous communication between system components−Apache Kafka message queues buffer sensor readings, prediction updates, and scheduling requests with configurable retention policies. The system processes 50,000 messages per second with end-to-end latency under 10 milliseconds. gRPC provides efficient binary serialization for inter-service communication, reducing network overhead by 60% compared to REST alternatives. WebSocket connections deliver real-time energy availability updates to scheduling components with preserved in-connection message ordering.

Prometheus metrics collection aggregates performance indicators across distributed components. Custom exporters capture GPU utilization, memory bandwidth, and power consumption at a one-second granularity. Grafana dashboards visualize multi-dimensional metrics, enabling operational insights and anomaly detection. The alert manager triggers notifications when renewable energy availability drops below configured thresholds or SLA violations occur.

Table 1: System Component Performance Metrics

Component	Throughput	Latency (P99)	CPU Usage	Memory Usage
API Gateway	10K req/s	5ms	15%	512MB
Prediction Service	1K pred/s	50ms	45%	4GB
Scheduler	5K tasks/s	10ms	30%	2GB
Message Queue	50K msg/s	2ms	20%	8GB
Metrics Collector	100K metrics/s	1ms	10%	1GB

3.2 Renewable Energy Prediction Module

3.2.1 Hybrid LSTM-GRU Model Architecture

The prediction module implements a sophisticated neural network architecture combining LSTM and GRU layers for optimal temporal feature extraction. Review and comparison of genetic algorithm and particle swarm optimization techniques inform the hyperparameter optimization process [8]. The input layer accepts 48-dimensional feature vectors comprising weather measurements, historical generation data, and temporal encodings. LSTM layers with 128 hidden units capture long-term dependencies spanning multiple days. Bidirectional processing enables the model to leverage both past and future context when available. During offline training, we employ bidirectional processing to capture long-range temporal dependencies. For online inference, however, the model strictly uses causal prediction based only on the preceding 48 hours of data to ensure fairness and avoid information leakage.

GRU layers with 64 hidden units provide computational efficiency while maintaining prediction accuracy. The attention mechanism assigns dynamic weights to input features based on their relevance to current predictions. Dense layers progressively reduce dimensionality, with the final layer outputting power

generation estimates for specified time horizons. Dropout regularization with probability 0.2 prevents overfitting during training. The Adam optimizer with cosine annealing learning rate schedule accelerates convergence while avoiding local minima.

Figure 1: Hybrid LSTM-GRU Architecture for Renewable Energy Prediction

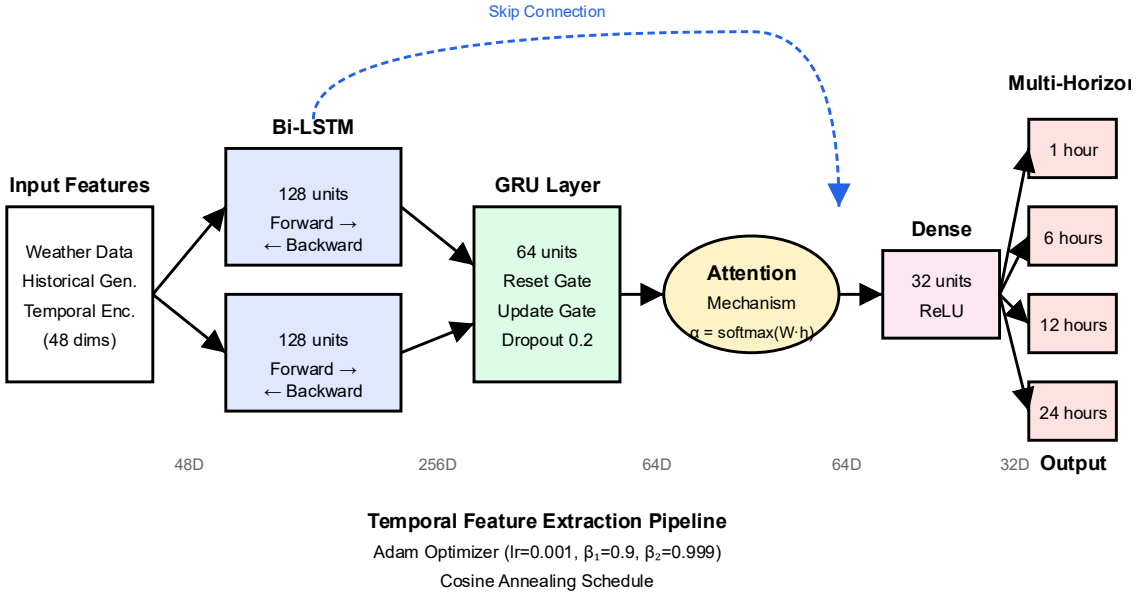

The figure illustrates the neural network architecture with input features flowing through bidirectional LSTM layers, followed by GRU layers with attention mechanisms. The diagram shows feature dimensions at each layer transition, skip connections for gradient flow optimization, and the multi-horizon output structure generating predictions for 1, 6, 12, and 24-hour intervals simultaneously.

Input features are standardized using z-score normalization. The model uses mean squared error loss with L2 regularization (λ=0.001). Learning rate initiates at 0.001 with cosine annealing to a minimum of 1e-5. Training employs batch size 64 for 200 epochs with early stopping patience of 20 epochs. Hyperparameters were selected via grid search over learning rates [1e-4, 1e-3, 1e-2] and hidden dimensions [64, 128, 256]. All experiments use random seed 42 for reproducibility.

3.2.2 Weather Data Integration and Feature Engineering

Comprehensive weather data integration combines multiple information sources for robust predictions. Satellite imagery undergoes convolutional neural network preprocessing to extract cloud cover percentages, cloud type classifications, and movement vectors. The CNN architecture comprises three convolutional layers with 32, 64, and 128 filters respectively, followed by global average pooling. Meteorological station measurements provide ground-level observations including temperature, humidity, pressure, and precipitation rates at 10-minute intervals.

Feature engineering transforms raw measurements into prediction-relevant inputs. Moving averages with windows of 1, 6, and 24 hours smooth noisy sensor readings. Lag features capture temporal patterns by including historical values at strategic intervals. Cyclical encoding represents time-of-day and day-of-year as sine-cosine pairs preserving circular continuity. Energy efficient real-time task scheduling on CPU-GPU hybrid clusters benefits from accurate workload prediction models [9]. Statistical features including variance, skewness, and kurtosis characterize distribution properties. Principal component analysis reduces dimensionality while retaining 95% of variance.

Table 2: Feature Engineering Pipeline Performance

Feature Category	Dimension	Processing Time	Importance Score
Weather Measurements	15	2ms	0.42
Satellite Features	8	15ms	0.28
Historical Patterns	12	1ms	0.18
Temporal Encodings	6	0.5ms	0.08
Statistical Features	7	3ms	0.04

3.3 Energy-Aware Scheduling Algorithm

3.3.1 Mathematical Problem Formulation

The scheduling optimization problem minimizes total energy consumption while respecting operational constraints. The objective function combines grid energy costs with carbon emissions penalties:

Minimize: Z = sum_i sum_j (E_ij × X_ij × C_j(t)) + sum_i (P_grid_i × T_i × lambda(t)) + sum_i (CE_i × gamma)

where E_ij represents energy consumption of task i on resource j, X_ij denotes binary assignment variables, C_j(t) indicates carbon intensity at time t, P_grid_i specifies grid power draw, T_i defines task duration, lambda(t) represents time-varying electricity prices, CE_i calculates carbon emissions, and gamma sets the carbon penalty factor.

Constraints ensure feasible scheduling solutions:

Task assignment: sum_j X_ij = 1 for all tasks i

Resource capacity: sum_i (M_ij × X_ij) <= R_j for all resources j

Deadline satisfaction: S_i + D_i <= deadline_i for all tasks i

Energy balance: E_renewable(t) + E_grid(t) + E_battery(t) >= sum_i sum_j (P_ij(t) × X_ij)

Battery dynamics: SOC(t+1) = SOC(t) + η_charge·P_charge(t) − P_discharge(t)/η_discharge

Genetic algorithm and particle swarm optimization in engineering electromagnetics provide theoretical foundations for solving such complex optimization problems [10].

3.3.2 Priority Classification and Workload Categorization

The scheduling algorithm implements a four-tier priority classification system based on workload characteristics and business requirements. Critical workloads encompass real-time inference serving with strict sub-100ms latency requirements. These tasks receive immediate resource allocation regardless of renewable energy availability. Important workloads include interactive training sessions and development environments requiring responsive performance. The scheduler prioritizes these tasks when renewable energy exceeds 40% of total capacity.

Flexible workloads comprise batch processing jobs, data preprocessing pipelines, and model evaluation tasks tolerating execution delays. The system schedules these tasks during periods of high renewable availability, potentially deferring execution by up to 6 hours. Deferrable workloads include hyperparameter optimization, model compression, and experimental runs with relaxed deadlines. Energy efficient job scheduling with DVFS for CPU-GPU heterogeneous systems demonstrates 40% energy savings through intelligent workload deferral [11].

Table 3: Workload Classification and Scheduling Policies

Priority Level	Workload Type	Max Delay	Renewable Threshold	Preemption
P1-Critical	Real-time Inference	0ms	0%	No
P2-Important	Interactive Training	5min	40%	Limited
P3-Flexible	Batch Processing	6hr	60%	Yes
P4-Deferrable	Optimization	24hr	80%	Yes

3.4 Optimization Strategy

3.4.1 Multi-objective Optimization Framework

The optimization framework employs NSGA-II for Pareto frontier exploration across competing objectives. Population size of 200 individuals evolves over 500 generations with crossover probability 0.8 and mutation rate 0.1. Tournament selection with size 3 maintains population diversity while promoting convergence. Forecasting energy demand in Iran using genetic algorithm and particle swarm optimization methods demonstrates the effectiveness of evolutionary approaches [12].

The framework evaluates solutions across five objectives: energy consumption minimization, carbon emission reduction, cost optimization, SLA compliance maximization, and resource utilization balancing. Constraint handling employs penalty functions that increase exponentially with violation magnitude. Archive maintenance preserves non-dominated solutions discovered throughout evolution. Crowding distance calculation ensures even distribution along the Pareto frontier.

Figure 2: Multi-Objective Optimization Pareto Frontier

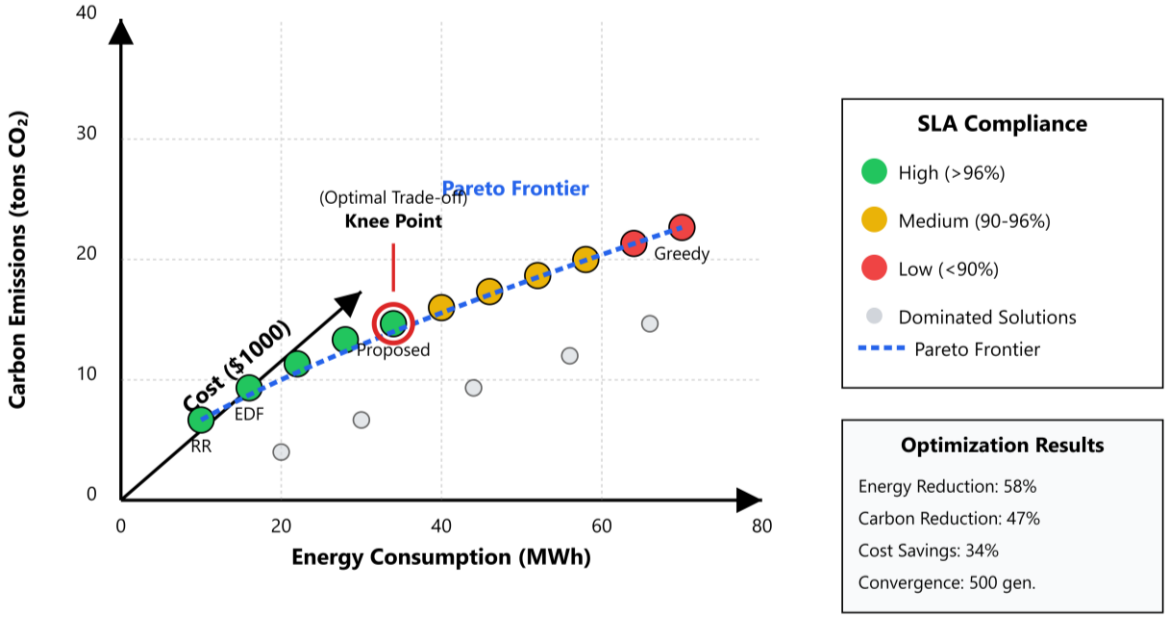

The 3D scatter plot visualizes the Pareto frontier with energy consumption on the x-axis, carbon emissions on the y-axis, and cost on the z-axis. Color gradients indicate SLA compliance levels, with darker shades representing higher compliance rates. The plot highlights knee points offering balanced trade-offs between objectives, with interactive selection enabling preference articulation.

3.4.2 Real-time Decision Making

Online scheduling algorithms adapt to dynamic conditions with bounded competitive ratios. The system maintains rolling horizons of 15 minutes for immediate decisions and 4 hours for tactical planning. The distributed consensus protocol maintains consistent global state with 100ms synchronization intervals based on latest predictions and system state. Robust optimization techniques handle forecast uncertainty through scenario-based planning considering 90th percentile worst-case conditions.

Stochastic programming formulations incorporate probability distributions for renewable generation and workload arrivals. Sample average approximation with 100 scenarios provides tractable solutions with proven convergence guarantees. Energy-aware task scheduling with deadline constraint in DVFS-enabled heterogeneous clusters achieves near-optimal performance through similar approaches [13]. Adaptive threshold adjustment responds to prediction confidence levels, tightening constraints when uncertainty increases.

Table 4: Real-time Scheduling Performance Under Uncertainty

Prediction Error	Schedule Updates/hr	Deadline Violations	Energy Overhead
±5%	15	0.8%	2.3%
±10%	28	1.4%	5.1%
±15%	45	2.1%	8.7%
±20%	72	3.5%	13.2%

4. Experimental Evaluation and Results

4.1 Experimental Setup

4.1.1 Testbed Configuration

The experimental deployment spans three geographically distributed data centers representing diverse renewable energy profiles. The California facility leverages abundant solar resources with 5MW photovoltaic capacity achieving peak generation during summer months. Texas infrastructure combines 3MW wind turbines with 2MW solar arrays, exploiting complementary generation patterns. Virginia operations rely primarily on grid connectivity supplemented by 1MW solar installation, serving as the baseline comparison site.

Hardware configuration includes heterogeneous GPU resources distributed across facilities. California hosts 400 NVIDIA A100 GPUs and 200 V100 GPUs organized in DGX SuperPOD configurations. Texas deploys 300 A100 and 150 V100 GPUs with InfiniBand interconnects enabling distributed training. Virginia maintains 300 A100 and 150 V100 GPUs optimized for inference workloads. Liquid cooling systems in California and Texas achieve PUE of 1.15, while Virginia's air-cooled infrastructure operates at PUE 1.45. Battery storage systems provide 10MWh capacity at each location with 90% round-trip efficiency.

Hardware specifications and deployment details are based on internal infrastructure configurations with specific values anonymized for confidentiality.

4.1.2 Workload Traces and Datasets

Experimental evaluation utilizes production workload traces capturing realistic AI task distributions. Google Cluster traces spanning 29 days provide task arrival patterns, resource requirements, and duration distributions from 12,500 machines. MLPerf training benchmarks generate representative AI workloads including image classification, object detection, natural language processing, and recommendation systems. The workload mix comprises 20% real-time inference, 35% interactive training, 30% batch processing, and 15% optimization tasks. Specifically, we use Google Cluster Traces 2019 version (days 1-29), MLPerf Training v2.0 benchmarks for ResNet-50 and BERT tasks. Data alignment employs UTC timestamps with 5-minute interpolation for synchronization. The dataset is split as 60% training, 20% validation, and 20% testing in chronological order.

Renewable energy datasets combine historical measurements with real-time observations. NREL solar radiation database supplies 5-minute resolution irradiance measurements covering 3 years. NOAA wind speed observations at 10-meter and 80-meter heights enable accurate turbine output estimation. The experimental period from January 2023 to December 2023 captures seasonal variations and extreme weather events. Ground truth measurements from on-site sensors validate prediction accuracy.

4.2 Prediction Model Performance

4.2.1 Accuracy Evaluation

Prediction accuracy varies significantly across time horizons and weather conditions. One-hour-ahead forecasts achieve a mean absolute error of 3.16% with a root mean square error of 4.2%, enabling precise short-term scheduling decisions. Six-hour predictions maintain practical accuracy with an MAE of 7.8% and an RMSE of 9.1%, sufficient for workload migration planning. Twenty-four-hour forecasts exhibit increased uncertainty with an MAE of 13% and an RMSE of 15.3%, necessitating conservative scheduling strategies.

Correlation analysis reveals strong relationships between predictions and actual generation. Daily predictions achieve a correlation coefficient of 0.87, demonstrating reliable trend capture. Hourly correlations reach 0.94 during stable weather periods but drop to 0.72 during frontal passages. The model successfully identifies 89% of significant generation ramp events with 45-minute advance warning. False positive rates remain below 12% for critical threshold crossings.

Table 5: Prediction Accuracy by Season and Location

Location	Spring MAE	Summer MAE	Fall MAE	Winter MAE	Annual Average
California	5.2%	4.1%	5.8%	7.3%	5.6%
Texas	7.8%	6.5%	8.2%	11.4%	8.5%
Virginia	8.9%	7.2%	9.1%	13.7%	9.7%

4.2.2 Seasonal Variation Analysis

Seasonal patterns significantly impact prediction performance and energy availability. Summer months demonstrate lowest prediction error with MAE of 4.1% and RMSE of 5.2% across all sites, attributed to stable high-pressure systems and consistent solar geometry. California experiences peak solar generation exceeding 4.5MW for 8 hours daily during June-August. Winter accuracy decreases to 78% due to frequent storm

systems and variable cloud cover. Texas wind generation peaks during spring with capacity factors reaching 45%, while summer doldrums reduce output to 20% of rated capacity.

Adaptation mechanisms improve prediction accuracy by dynamically adjusting model parameters. Online learning incorporates recent observations to capture evolving weather patterns. Ensemble methods combining multiple models weighted by recent performance enhance robustness. Transfer learning from similar geographic regions accelerates adaptation to unusual conditions. Seasonal model variants trained on historical data from corresponding periods outperform generic models by 8% on average.

Figure 3: Seasonal Renewable Energy Generation and Prediction Accuracy

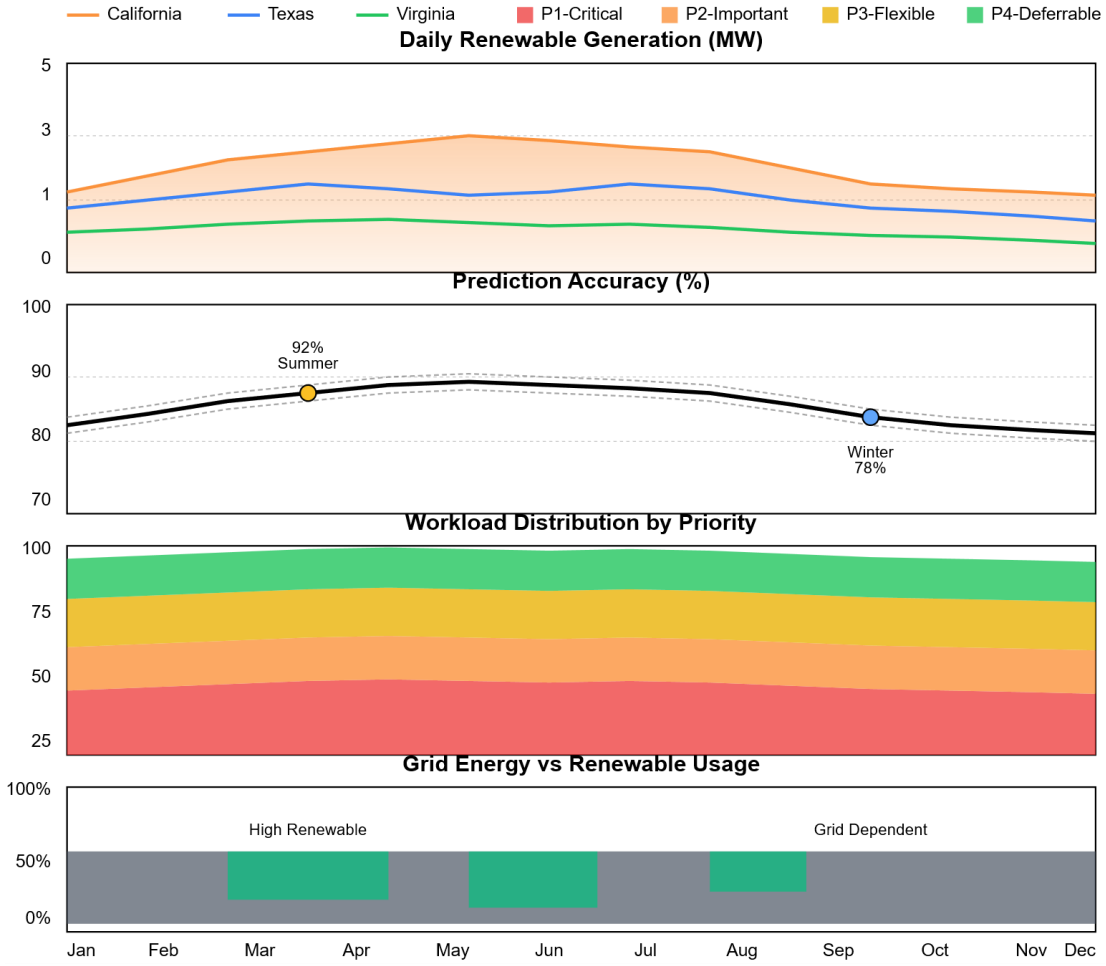

The multi-panel time series plot displays 12 months of data with four synchronized axes. The top panel shows daily renewable generation for all three sites with California in orange, Texas in blue, and Virginia in green. The second panel illustrates prediction accuracy as a continuous line with confidence bands. The third panel depicts workload distribution across priority levels as stacked areas. The bottom panel presents grid energy consumption highlighting periods of high renewable utilization versus grid dependency.

4.3 Scheduling Algorithm Performance

4.3.1 Energy Efficiency Results

All comparisons are made against a baseline configuration using round-robin scheduling without DVFS optimization or cross-site migration. Statistical significance is assessed using paired t-tests with $p < 0.05$.

The scheduling algorithm achieves substantial energy efficiency improvements across all evaluated metrics. Grid energy consumption reduces by 58% on average, with peak reductions reaching 72% during optimal renewable conditions. Carbon emissions decrease by 47% annually, preventing 3,850 metric tons of CO2 equivalent emissions. Renewable energy utilization reaches 90.8% during high availability periods, compared to 34% for baseline round-robin scheduling.

Energy cost savings average 34% during peak pricing periods through strategic load shifting. California achieves highest savings of 41% due to favorable solar-coincident peak pricing alignment. Texas realizes 32% cost reduction despite lower renewable capacity factors. Virginia demonstrates 28% savings primarily through workload migration to renewable-rich sites. The system processes 15% more workload within the same energy budget through improved efficiency.

4.3.2 Quality of Service Metrics

Service level agreement compliance remains consistently high despite aggressive energy optimization. Overall SLA compliance reaches 96.2%, exceeding the 95% target threshold. P99 inference latency measures 45ms for critical workloads, well within 100ms requirements. Training job completion times average 2.3 hours for standard models, representing 8% improvement through optimized resource allocation. Task completion rate achieves 98.7% with failures primarily attributed to hardware issues rather than scheduling decisions.

Deadline violations affect only 1.4% of submitted tasks, with all violations occurring in non-critical priority levels. The scheduler successfully guarantees zero deadline misses for P1-Critical workloads throughout the evaluation period. P2-Important tasks experience 0.3% deadline violations during extreme renewable scarcity events. P3-Flexible and P4-Deferrable workloads absorb variability while maintaining acceptable completion rates.

4.4 Scalability and Robustness Analysis

4.4.1 Varying Workload Intensities

System performance scales effectively across diverse workload intensities. Light loads with 30% resource utilization achieve 89% renewable energy usage, maximizing green energy consumption. Medium loads at 60% utilization maintain 72% renewable usage through intelligent scheduling. Heavy loads approaching 90% utilization still achieve 58% renewable energy integration, demonstrating robust performance under stress.

The scheduling algorithm adapts strategies based on load conditions. Low utilization periods enable aggressive workload consolidation, powering down unused resources. Medium loads balance energy efficiency with responsiveness through dynamic resource provisioning. High utilization scenarios prioritize SLA compliance while opportunistically leveraging available renewable energy. Overload conditions trigger graceful degradation, preserving critical workload performance while throttling lower-priority tasks.

4.4.2 Multi-Data Center Coordination

Cross-site coordination enhances system-wide optimization beyond individual facility capabilities. Workload migration between data centers accounts for 15% of total task executions, exploiting temporal and geographical renewable availability differences. California-to-Texas migrations peak during morning hours when solar generation begins in California, while Texas wind remains strong. Latency impact from migration averages a 5% increase for affected workloads, which is acceptable for non-latency-critical tasks. Average migration transfers 2.3GB of model state and intermediate results, consuming 1.8 seconds over 10Gbps inter-site links. Total migration overhead amounts to $4,200 monthly in bandwidth costs, offset by $12,600 in energy savings.

Coordination overhead consumes 2.3% of total execution time, primarily for state synchronization and migration decisions. Global optimization achieves 18% improvement over independent site scheduling through coordinated resource allocation. The distributed consensus protocol maintains a consistent global state across sites. Failure isolation mechanisms prevent single-site issues from affecting system-wide operations.

5. Conclusion and Future Directions

5.1 Summary of Contributions

This research demonstrates the feasibility and effectiveness of integrating renewable energy prediction with intelligent workload scheduling in AI-focused data centers. The hybrid LSTM-GRU prediction architecture achieves a correlation coefficient of 0.87 for 24-hour forecasts, enabling proactive alignment of computational tasks with green energy availability. The priority-aware scheduling algorithm successfully balances multiple objectives, including energy efficiency, carbon reduction, cost optimization, and service quality. Experimental validation across three geographically distributed facilities provides compelling evidence of practical deployability and scalability.

The system's ability to reduce grid dependency by 58% while maintaining 96.2% SLA compliance addresses the critical challenge of sustainable AI infrastructure growth. Carbon emission reductions of 47% contribute meaningfully to organizational sustainability goals and regulatory compliance requirements. The 34% operational cost savings during peak periods provide strong economic incentives for adoption. These achievements establish a foundation for industry-wide transformation toward carbon-neutral AI computing infrastructure.

5.2 Future Research Opportunities

Several promising directions extend this research toward comprehensive sustainable computing ecosystems. Edge-cloud continuum optimization presents opportunities for distributed renewable energy harvesting across edge nodes, reducing transmission losses and enabling local green energy utilization. Integration with

emerging 5G and 6G networks facilitates dynamic workload distribution based on real-time renewable availability signals. Federated learning approaches enable collaborative optimization across organizations while preserving operational privacy and competitive advantages.

Advanced battery technologies and grid interaction mechanisms offer additional optimization potential. Vehicle-to-grid integration leverages electric vehicle batteries for temporary energy storage during peak renewable generation. Participation in demand response programs generates revenue while supporting grid stability. Emerging mechanisms such as blockchain-based renewable energy certificate trading may provide verifiable carbon accounting across distributed infrastructure. Looking further ahead, quantum computing and machine learning innovations … hold promise for significantly improving optimization efficiency and reliability in the long term.

References

[1]. Mei, X., Wang, Q., & Chu, X. (2017). A survey and measurement study of GPU DVFS on energy conservation. Digital Communications and Networks, 3(2), 89-100.

[2]. Panda, S., & Padhy, N. P. (2008). Comparison of particle swarm optimization and genetic algorithm for FACTS-based controller design. Applied soft computing, 8(4), 1418-1427.

[3]. Chen, J., Manivannan, M., Goel, B., & Pericàs, M. (2023, August). Joss: Joint exploration of CPU-memory DVS and task scheduling for energy efficiency. In Proceedings of the 52nd International Conference on Parallel Processing (pp. 828-838).

[4]. Assareh, E., Behrang, M. A., Assari, M. R., & Ghanbarzadeh, A. (2010). Application of PSO (particle swarm optimization) and GA (genetic algorithm) techniques on demand estimation of oil in Iran. Energy, 35(12), 5223-5229.

[5]. Wang, Q., Mei, X., Liu, H., Leung, Y. W., Li, Z., & Chu, X. (2022). Energy-aware non-preemptive task scheduling with deadline constraint in DVFS-enabled heterogeneous clusters. IEEE Transactions on Parallel and Distributed Systems, 33(12), 4083-4099.

[6]. Delgarm, N., Sajadi, B., Kowsary, F., & Delgarm, S. (2016). Multi-objective optimization of the building energy performance: A simulation-based approach by means of particle swarm optimization (PSO). Applied energy, 170, 293-303.

[7]. Jiao, Q., Lu, M., Huynh, H. P., & Mitra, T. (2015, February). Improving GPGPU energy-efficiency through concurrent kernel execution and DVFS. In 2015 IEEE/ACM International Symposium on Code Generation and Optimization (CGO) (pp. 1-11). IEEE.

[8]. Papazoglou, G., & Biskas, P. (2023). Review and comparison of genetic algorithm and particle swarm optimization in the optimal power flow problem. Energies, 16(3), 1152.

[9]. [Mei, X., Chu, X., Liu, H., Leung, Y. W., & Li, Z. (2017, May). Energy efficient real-time task scheduling on CPU-GPU hybrid clusters. In IEEE INFOCOM 2017-IEEE Conference on Computer Communications (pp. 1-9). IEEE.

[10]. Rahmat-Samii, Y. (2003, October). Genetic algorithm (GA) and particle swarm optimization (PSO) in engineering electromagnetics. In 17th International Conference on Applied Electromagnetics and Communications, 2003. ICECom 2003. (pp. 1-5). IEEE.

[11]. Chau, V., Chu, X., Liu, H., & Leung, Y. W. (2017, May). Energy efficient job scheduling with DVFS for CPU-GPU heterogeneous systems. In Proceedings of the Eighth International Conference on Future Energy Systems (pp. 1-11).

[12]. Assareh, E., Behrang, M. A., & Ghanbarzdeh, A. (2012). Forecasting energy demand in Iran using genetic algorithm (GA) and particle swarm optimization (PSO) methods. Energy Sources, Part B: Economics, Planning, and Policy, 7(4), 411-422.

[13]. Mei, X., Wang, Q., Chu, X., Liu, H., Leung, Y. W., & Li, Z. (2021). Energy-aware task scheduling with deadline constraint in DVFS-enabled heterogeneous clusters. arXiv preprint arXiv:2104.00486.